J Nanostruct 16(4): 5434-5450, Autumn 2026

RESEARCH PAPER

Evaluation of the Antibacterial and Antibiofilm Activity of Selenium Nanoparticles Against Gram-Positive and Gram-Negative Bacteria

*Ruwaidah Abdulameer Mussttaf [1], Thanaa Rasheed Abdulrahman [2], Ayat Adheem Kadim [1] **

[1] *Department of Physiology and Medical Physics College of Medicine, Al-Nahrain University, Iraq*

[2] *Department of Medical Microbiology, College of Medicine, Al-Nahrain University, Iraq*

ARTICLE INFO

Article History:
Received 20 June 2026
Accepted 16 September 2026
Published 01 October 2026

Keywords:
Antibacterial
Antibiofilm
Gram negative
Gram positive
Se NPs

ABSTRACT

The emergence of antibiotic resistance bacteria is amajor concern for public health that threatens to outpace development of new effective drugs for infection control, the metal selenium(Se) has got much attention in the last years because it stable under diverse environmental conditions. Synthesized Se NPs by use plant extract (allium sativum) , Study of the structural and morphological properties, as well as the optical and biological properties (such as UV-Vis spectroscopy ,FTIR,XRD,FESEM and EDX), Using the nano-extract as an antibacterial agent against some types of pathogenic bacteria such as (*Staphylococcus aureus* and *Escherichia coli*) using well diffusion method.Evaluation the antibiofilm effect of biosynthesized tin oxide and selenium nanoparticles against (*Staphylococcus aureus* and *Escherichia coli).* Se NPs was synthesized via a green synthesis approach using garlic extract as a reducing and stabilizing agent. The synthesized nanoparticles were characterized using X-ray diffraction (XRD), field emission scanning electron microscopy (FESEM), energy-dispersive X-ray spectroscopy (EDX), atomic force microscopy (AFM), Fourier-transform infrared spectroscopy (FTIR), UV–Visible spectroscopy, and zeta potential analysis. Antibacterial activity was assessed by the agar well diffusion method against clinical isolates of Escherichia coli and *staphylococcus* aureus. Biofilm-forming ability was evaluated using the microtiter plate assay, and antibiofilm activity was determined by measuring the reduction in biofilm biomass following nanoparticles treatment. XRD analysis confirmed the successful formation of crystalline SeNPs the average crystallite sizes 17.6, respectively. FESEM analysis revealed average particle sizes of 17.67 nm for SeNPs. EDX results confirmed the high purity of both nanoparticles, while zeta potential analysis demonstrated good colloidal stability with negative surface charges ranging between −30 and −40 mV. Optical studies revealed strong absorption characteristics and an optical band gap of approximately 2.75 eV. Biological evaluation showed that SeNPs exhibited concentration dependent antibacterial activity against both *E. coli* and *S. aureus*, with stronger activity against *S. aureus*. SeNPs exhibited antibiofilm activity with mean inhibition percentages of 17.49% against *E. coli* and 36.42% against *S. aureus*. The present study successfully synthesized stable and highly crystalline SeNPs through an environmentally friendly green synthesis approach using garlic extract. SeNPs demonstrated significant antibacterial and moderate antibiofilm activities, particularly against S. aureus. These findings suggest that green-synthesized SeNPs may serve as promising candidates for controlling biofilm-associated infections and combating antimicrobial resistance in wound and burn pathogens.

How to cite this article
Mussttaf R., Rasheed T., Kadim A. Evaluation of the Antibacterial and Antibiofilm Activity of Selenium Nanoparticles against Gram-Positive and Gram-Negative Bacteria. J Nanostruct, 2026; 16(4):5434-5450. DOI: 10.22052/JNS.2026.04.077

* *Corresponding Author Email: ayat.a.kadhim.mphy24@ced.nahrainuniv.edu.iq*

INTRODUCTION

The word nano is derived from the Greek word "nanos," meaning "very short man." The International Organization for Standardization (ISO), an international organization for classical metrology, defines it as a differential material (nanomaterial, NM) with an internal or surface structure within the differential scale, or an external radius on the nanoscale. A nanomember whose three external radiifall within the differential scale (from 1 to 100 overall) is also referred to as a differential particle (nanoparticle, NP) [1].

The era of nanotechnology began in 1959 with Richard Feynman's ideas on controlling individual atoms, "there is plenty of room at the bottom [2].

Materials at the molecular and atomic levels, with sizes between 0.1 and 100 nanometers, are the focus of nanotechnology. The particles' small size gives them many benefits in contemporary medicine, such as drug delivery with fewer adverse effects [3]. Because of their extremely small size, nanoparticles have unique physical, chemical, and biological properties that are not present in larger materials. They are invisible to the human eye because of their submicron size. These features, which include a higher surface area-to-volume ratio, quantum effects, high reactivity, and the ability to penetrate biofilms, make them desirable choices for a variety of biomedical applications [4].

Nanomedicine is a branch of nanotechnology, and it is considered one of the promising fields for treating and preventing diseases, Owing to its distinctive physical and chemical properties. The term "nano" refers to extreme smallness, so nanomedicine focuses on drug formulations at the nanoscale (nanoparticles). These nanoparticles can be used to deliver a wide range of therapeutic drugs via encapsulation [5].

In the medical field, Se acquires a unique place [6]. Several enzymes that are involved in processes like antioxidation, detoxification, and metabolism, such as glutathione peroxidases (GPx), iodo-thyronine deiodinases, and thioredoxin reductase (TrxR), contain selenium [7,8].

Various selenium oxyanions (selenite, selenite or selenide) can be toxic to human and animal cell lines. Elemental selenium (Se^0) under biological Toxicity was not demonstrated at concentrations below 400 µg/mL. In addition, Selenium is present in organic forms like selenocysteine (Secys) and inorganic form of selenomethionine (Semet) that includes selenite ($SeO3^{-2}$), selenate ($SeO4^{-2}$) and selenide (Se^{-2}) [9]. SeNPs exhibited outstanding antimicrobial properties against Streptococcus and Candida albicans [10], Staphylococcus aureus [11] and mutans [12]. Additionally, the SeNPs' biological properties, such as their antibacterial, low-toxicity antiviral and antioxidant activity on human cells have offered a field for investigation in nanotechnology [13,14].

The difference in structures of Gram-positive and Gram-negative bacteria plays an important role in the susceptibility of these bacteria towards antimicrobial agents such as nanoparticles. Gram-negative bacteria have an outer membrane that contains lipopolysaccharides, providing an extra protective barrier to restrict the penetration of external compounds.

Characterization tools such as transmission electron microscopy (TEM), X-ray diffraction spectroscopy (XRD), Fourier transform infrared spectroscopy (FTIR), ultraviolet-visible spectroscopy (UV-vis), atomic force microscopy (AFM) and zeta potential (ZP) can be used to closely examine these properties such as size, shape, surface characteristics, and other physiological features [16].

Biofilms are intricate microbial communities which can be problematic in many fields such as industry, environment and human health. Because of the protective nature of biofilms, they are able to resist against conventional anti-biofilm strategies including chemical agents, mechanical interventions and surface modifications. In order to overcome the limitations of the traditional approaches, several emerging strategies have been explored such as the use of natural compounds, nanotechnology based techniques, quorum-sensing inhibition, enzymatic degradation and antimicrobial photodynamic or sonodynamic therapy. Recently, the use of more than one anti-biofilm approach has been explored to improve treatment effectiveness and to prevent microbial resistance. Therefore, the mechanisms by which biofilms form and novel strategies to overcome the shortcomings of traditional anti-biofilm strategies continue to be studied [17].

Escherichia coli (E. coli) is a Gram-negative, non–spore-forming bacterium that is typically motile by peritrichous flagella. It was first described by Theodor *Escherich* in 1885. *E. coli* is considered a normal component of the intestinal microbiota of humans and animals. As part of the normal flora, most *E. coli* strains colonize the gastrointestinal

tract of humans and animals without causing disease [18].

However, certain strains of *E. coli* have evolved into pathogenic forms through the acquisition of virulence factors carried by plasmids, transposons, bacteriophages, or pathogenicity islands. Pathogenic *E. coli* can be classified according to their serogroups, mechanisms of pathogenicity, clinical manifestations, or virulence factors [19].

The adaptable Gram-positive *Staphylococcus* aureus is a facultative anaerobic bacterium that can function as both an opportunistic pathogen and a commensal organism resulting in a wide range of illnesses in humans [22].

Among the most clinically important bacterial pathogens, which cause infections that range from superficial skin to (SSTIs) to potentially fatal illnesses like *pneumonia, endocarditis, osteomyelitis, septic* bacteremia and arthritis [23].

S. aureus is a versatile and robust organism that colonizes the surfaces of the skin, mucosa and anterior nares in approximately 30% of the healthy population, but can exploit host barriers or immune defenses to cause invasive infections [24].

The main factor contributing to S. aureus's pathogenic success is its high level of virulence elements, allowing it to stick to host tissues, avoid immunological reactions, and harm host cells [25].

Surface-associated proteins like fibronectin-binding and clumping factors (ClfA, ClfB) Adhesion to host cells and tissues is facilitated by proteins. At the same time, the toxins released, including Panton-Valentine leukocidin (PVL), α-hemolysin, and toxic shock syndrome toxin-1 (TSST-1), contribute to the systemic toxicity and tissue damage [26].

Additionally, its capacity to create strong biofilms on prosthetic implants and medical equipment increases persistence by protecting bacteria from host defenses and antimicrobial agents, causing chronic and recurrent infections [27].

The extraordinarily complex nature of *S. aureus* infections complicates their clinical management ability to develop and acquire resistance to antibiotics. The advent of methicillin. In both community and medical settings, resistant *S. aureus* (MRSA) has made many Global rates of morbidity and mortality have increased due to the ineffectiveness of first-line antibiotics [28].

Over the past few decades, strains that are less susceptible to vancomycin (VRSA) and resistance the pathogen's evolutionary adaptability was demonstrated by its resistance to last-resort antibiotics [29].

Recognizing the molecular and genetic processes underlying antibiotic resistance and the development of new therapeutics requires an understanding of the evolutionary dynamics of resistant strains. methods and public health tactics [30,31].

MATERIALS AND METHODS

This study was conducted from 16th of December 2025, to the end of May 2026. A total of sixteen bacterial isolates were collected from various clinical specimens from different wounds and burn swabs. Preliminary identification was performed using conventional microbiological methods, and the results were subsequently confirmed using the Vitek 2 system at the laboratories of Al-Zahraa Teaching Hospital in Wasit.

In this study, selenium (Se) nanoparticles was synthesized using a green synthesis approach. Garlic (Allium sativum) extract was utilized as a reducing and stabilizing agent. The synthesis procedure was carried out in the Department of Physics at Wasit University.

The synthesized nanoparticles were characterized using several analytical techniques, including UV–Visible spectroscopy (UV–Vis), X-ray diffraction (XRD), Fourier transform infrared spectroscopy (FTIR), (FESEM), and atomic force microscopy (AFM).

Furthermore, the antibacterial activity of the synthesized nanoparticles was evaluated, along with their inhibitory effect on biofilm formation. All experiments were conducted in the Department of Microbiology, College of Medicine, Al-Nahrain University.

Green Synthesis Method

Metal nanoparticles tin oxide &selenium were prepared by using Allium Sativum (garlic)extract through a green synthesis approach by reduction of metallic salts with aqueous solution of leaf extract.

Preparation of Aqueous Leaf Extract

1. Weigh approximately 20 g of peeled garlic cloves.

2. Grind the cloves in a mortar and pestle (or blender) with a small amount of DI water to obtain

a coarse paste.

3.The garlic paste was transferred into a 250 mL beaker and DI water was added to reach a total volume of 200 mL.

4. The mixture was heated to 60–70 °C on a hot plate under gentle magnetic stirring for 20–30 min (avoid boiling).

5. Subsequently, the mixture was allowed to cool to room temperature and was filtered through Whatman No. 1 filter paper to remove solid residues.

7. The clear filtrate was collected in a clean container and stored at 4 °C 8. The extract was used within 24–48 h to ensure optimum reducing and capping activity.

Preparation of Selenium NPs

Selenium nanoparticles were synthesized using the green synthesis method with Garlic aqueous extract as a reducing and stabilizing agent:

Initially, a 20 mM Na_2SeO_3 working solution was prepared by diluting the 1.0 M stock.

Specifically, 2.0 mL of 1.0 M Na_2SeO_3 was mixed with 98.0 mL of deionized (DI) water to obtain a total volume 100 mL

Subsequently, 50 mL of the prepared 20 mM Na_2SeO_3 solution was transferred working solution into a 250 mL conical flask.

Under magnetic stirring at room temperature, 5–10 mL of garlic extract was added dropwise to the selenite solution.

The volume ratio between the Na_2SeO_3 solution and garlic extract was maintained within the range of approximately ≈ 10:1 to 5:1.

The pH of the reaction mixture was measured and adjusted to approximately pH 7.0–8.0 by the dropwise addition of 0.1–0.5 M HCl under stirring.

the reaction mixture was then heated to 50–60 °C and maintain at this temperature for 2–4 h with continuous stirring.

The formation of elemental selenium Se^0 nanoparticles was monitored by the observed color change of the solution, which turned orange, brick red or reddish brown with time.

Upon finishing the reaction, the reaction mixture was let cool to room temperature.

The formed colloidal suspension was then poured into the centrifuge tubes and centrifuged at 4000–8000 rpm for 15–20 min to separate out the Se NPs.

The supernatant was carefully removed and the pellet collected was re-dispersed in DI water.

The washing and centrifugation were repeated at least three times to remove any remaining ions and excess garlic derived components.

The finally, the purified SeNPS pellet was transferred to a clean glass dish and dried in a hot air oven at 40–60 °C for several hours until a dry SeNPS powder is obtained.

The dried SeNPs were gently ground using an agate mortar to produce a fine powder and were subsequently stored in an airtight amber vial at room temperature for further characterization and antibacterial evaluation.

Measuring Device

The Tin oxide and Selenium nanoparticles that synthesized by green synthesis method were characterizes through UV-VIS spectroscopy, XRD, FTIR, TEM, SEM and Zeta potential.

Preparation of Culture Media

The culture media was prepared in accordance with the manufacturer's instructions, and the culture media solution in the beaker was autoclaved for 15 minutes at 121°C and 15 pounds per square inch to sterilize it. After that, remove it from the autoclave and poured into Petri-dishes or universal tubes until it warms up. Then stored in a refrigerator at 4°C until needed.

Muller Hinton Agar

This medium was prepared by dissolving 38 g in 1000 ml of distilled water, autoclaved for 15 minutes at 121°C. Later, cooled to 50°C, poured into petri dishes and then establish at room temperature. Preserved at the refrigerator until used.

Brain Heart Infusion Broth

The Broth medium was prepared by dissolving 37 g in 1000 ml of distilled water, autoclaved for 15 minutes at 121°C ,15 pounds per square inch for 15 minutes. The Broth was poured into the penal tubes and kept at 4°C until be used.

Luria-Bertani Broth

The following unique additions are needed for this medium: One liter of distilled water was used to dissolve 10 grams of tryptone, 10 grams of Na Cl, and 5 grams of yeast extract. LB broth was then prepared as a 3 milliliter aliquot in test tubes, autoclaved, and stored at 4°C until it was needed for activation isolates and the biofilm formation

test.

Preparation of solutions

McFarland's Standard (0.5)

The most widely used standard in clinical microbiology is the 0.5 McFarland Standard. The 0.5 McFarland suspension of bacteria in Luria Bertani Broth was prepared by mixing 5µl of bacteria suspensions with 3ml of Luria Bertani Broth by using Micropipettes. It is best to use it on the same day of preparation.

Preparation and Standardization of the Bacterial Inoculum

Four to five pure colonies were used. The inoculum was prepared by either diluting a broth culture or emulsifying overnight colonies grown on an agar medium. The broth used was not incompatible with the antimicrobial agent being tested. For visual comparison, the suspension was adjusted to a density of approximately 1.5×10^8 CFU/ml by comparison with a 0.5 McFrland standard. To minimize variations in inoculum density, the plates were inoculated within 30 minutes after standardization of the inoculum [32].

Antibacterial Effect of Nanoparticles against Staphylococcus aurous and Escherichia coli

The antibacterial effect of the Selenium nanoparticles was assessed by well diffusion method as follows:

1- A hole was make with a diameter of (7 mm) by punch aseptically with a sterile cork borer or a tip into the Muller Hinton Agar plates.

2- The sterile cotton swab was dipped into the standardized bacterial solution and carefully pressing the swab against the tube wall at a level above the liquid to remove excess bacteria suspension.

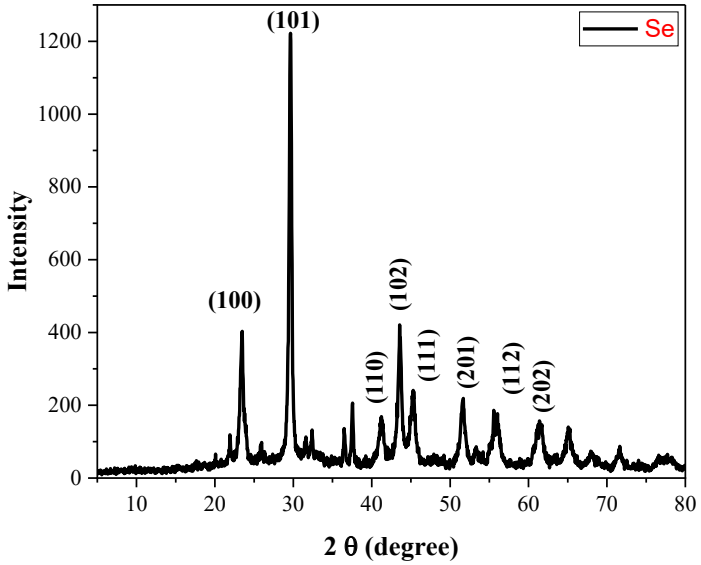

Fig. 1. X-ray diffraction (XRD) pattern of (SeNPs).

Table 1. FTIR absorption bands and corresponding functional group assignments of green-synthesized SeNPs using garlic extract.

Wavenumber (cm^{-1})	Functional Group / Bond	Assignment
3400	O-H stretching	Hydroxyl groups of phenols, alcohols, and adsorbed water
2920	C-H stretching	Aliphatic alkane groups from organic biomolecules
1630-1650	H-O-H bending / C=O / Amide	Adsorbed water and biological organic compounds
1450-1380	C-N / C-H bending	Organic phytochemical compounds from garlic extract
1250-1050	C-O / C-S stretching	Alcoholic, sulfur-containing, and organosulfur compounds
950-800	Se-O / organic skeletal vibrations	Residual selenium-related surface interactions
700-500	Se-Se vibration	Characteristic vibration of elemental selenium nanoparticles

3- The culture bacteria solution in the swab was wiped on agar plates, a different swab for each petri dish.

4-Then, 50 µl of each nanoparticles with different concentration was placed into each well by using Micropipettes.

5- Finally, the agar plates were incubated for 24 hours at 37 °C and inhibition of growth was examined by diameter calculation of clear zone surrounding each well.

Antibiofilm Activity of Selenium nanoparticles

A modified microtiter plate (MTP) assay was used to assess the antibiofilm activity of selenium nanoparticles (SeNPs) against *Staphylococcus aureus* and *Escherichia coli* [33]. In this experiment, two different sterile 96-well microtiter plates were utilized. Under the same experimental conditions, the plate was used to treat SeNPs. In short, each well was inoculated with 100 µL of bacterial suspension made in LB broth, and then nanoparticles were added at a final concentration of 100 $\mu g \cdot mL^{-1}$. To get rid of non-adherent (planktonic) cells, the wells were rinsed three times with physiological saline following incubation. After 20 minutes of methanol fixation and air drying, the attached biofilm cells were stained for another 20 minutes with 0.5% (w/v) crystal violet. The bound dye was then dissolved by adding 200 µL of 33% (v/v) acetic acid to each well for 30 minutes after the wells had been cleaned once more and allowed to air dry. Eliza reader was used to measure the absorbance at 595 nm.

Statistical Analysis

The obtained experimental data were analyzed using OriginPro 2021 software for data processing, graphical representation, curve fitting, and statistical evaluation of the structural, morphological, optical, and biological properties of the synthesized nanoparticles.

RESULTS AND DISCUSSION

Physical characterization

Structural Properties (X-ray diffraction)

The X-ray diffraction of Se NPS

the X-ray diffraction (XRD) pattern of selenium nanoparticles (SeNPs) synthesized via the green synthesis approach using garlic extract as a natural reducing and stabilizing agent. The diffraction peaks observed at approximately 23.43°, 29.63°, 41.25°, 43.59°, 45.28°, 51.62°, 55.63°, 61.48°, and 67.98° correspond to the crystallographic planes (100), (101), (110), (102), (111), (201), (112), (202), and related reflections of trigonal hexagonal selenium (t-Se), respectively (Fig. 1).

Fourier Transform Infrared Spectroscopy FTIR of Selenium nanoparticles (SeNPs)

Fig. 2 shows the FTIR spectrum of green-synthesized selenium nanoparticles (SeNPs) prepared using garlic extract as a natural reducing and stabilizing agent. Several characteristic

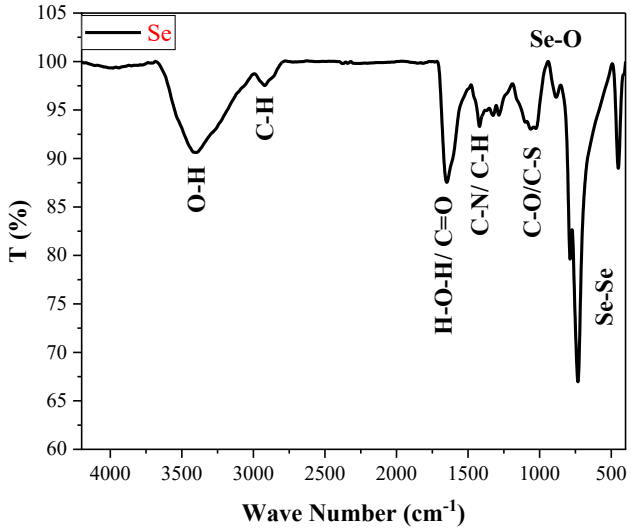

Fig. 2. FTIR of Selenium nanoparticles (SeNPs).

absorption bands were observed, confirming the presence of bioactive functional groups associated with the phytochemical compounds of garlic extract adsorbed on the surface of the synthesized nanoparticles. The broad absorption band centered around 3400 cm^{-1} is attributed to the stretching vibrations of hydroxyl groups (O-H) originating from phenolic compounds, adsorbed moisture, and biomolecules present in the garlic extract. The weak bands observed near 2920 cm^{-1} correspond to asymmetric and symmetric stretching vibrations of aliphatic (C-H) groups. The absorption band around 1630-1650 cm^{-1} can be assigned to the bending vibration of adsorbed water molecules and/or amide functional groups associated with biological organic compounds. The bands appearing in the region 1400-1000 cm^{-1} are related to (C-N), (C-O), and (C-S) stretching vibrations, indicating the interaction of sulfur-containing organometallic compounds from garlic extract with the selenium nanoparticle surface.

Morphological Properties

FESEM of Selenium nanoparticles (SeNPs)

The FESEM micrograph of green synthesized selenium nanoparticles (SeNPs) prepared using garlic extract as a natural reducing and stabilizing agent Fig. 3 shown. The image reveals the formation of densely distributed nanoparticles with semi-spherical to irregular granular morphology accompanied by slight agglomeration.

EDX spectrum and elemental mapping analysis of selenium nanoparticles (Se NPs)

Fig. 4 and Table 2 shown the EDX spectrum and elemental mapping analysis of green-synthesized selenium nanoparticles (Se NPs) prepared using garlic extract. The EDX spectrum confirms the successful formation of selenium nanoparticles through the appearance of strong characteristic selenium peaks, particularly the intense SeLα peak, together with a weak oxygen signal corresponding to surface-adsorbed oxygen-containing groups· There were no significant impurity peaks observed, which shows the high purity of the synthesized nanoparticles. The quantitative EDX analysis showed that the selenium is the major element in the prepared sample with a weight percentage of ~95.25 wt.% and an atomic percentage of ~80.24 at.%, while

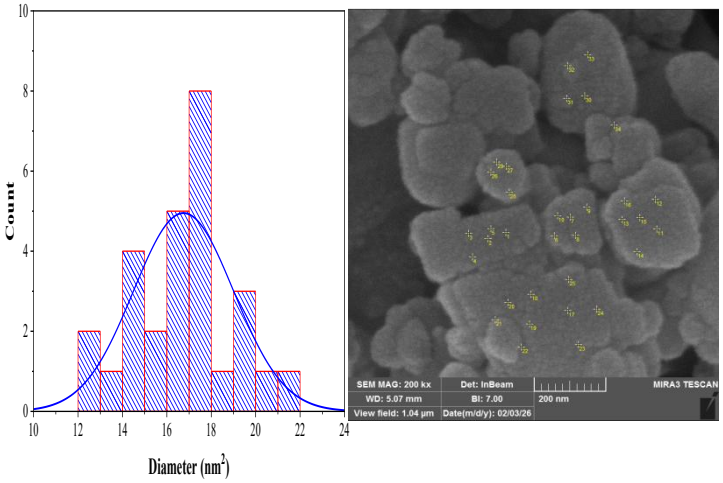

Fig. 3. The FESEM micrograph of green synthesized selenium nanoparticles.

Table 2. Quantitative EDX elemental composition of selenium nanoparticles (Se NPs).

Elt	Line	Int	Error	K	Kr	W%	A%	ZAF
O	Ka	20.5	25.8799	0.0160	0.0150	4.75	19.76	0.3163
Se	La	1196.7	45.2856	0.9840	0.9243	95.25	80.24	0.9703
				1.0000	0.9393	100.00	100.00	

oxygen has a weight percentage of ~4.75 wt.% and atomic percentage of ~19.76 at.%. The low amount of oxygen is due to the surface oxidation and/or possible adsorption of oxygen-containing phytochemical residues from the garlic extract used in the green synthesis process. The elemental mapping images also show that the selenium is relatively uniformly distributed throughout the area analyzed, suggesting that nucleation and dispersion of Se nanoparticles were successful without elemental segregation or agglomeration. The distribution intensity of oxygen mapping showed a relatively low degree of distribution, consistent with quantitative EDX results. This high selenium content along with uniform elemental distribution proves the effectiveness of garlic extract as a natural reducing and stabilizing agent in the synthesis of nanoparticles. The phytochemical compounds present in garlic might have played a role in controlling the growth of nanoparticles and preventing them from aggregating too much, possibly by capping their surfaces.

AFM of Selenium nanoparticles (SeNPs)

The AFM surface morphology of green synthesized selenium nanoparticles (SeNPs) using garlic extract is shown in Fig. 5. The AFM images show that the surface is relatively rough and non-uniform, with the presence of nanoscale grains and surface features that are clustered together. The three dimensional topography confirms the formation of granular nanostructures with distinct

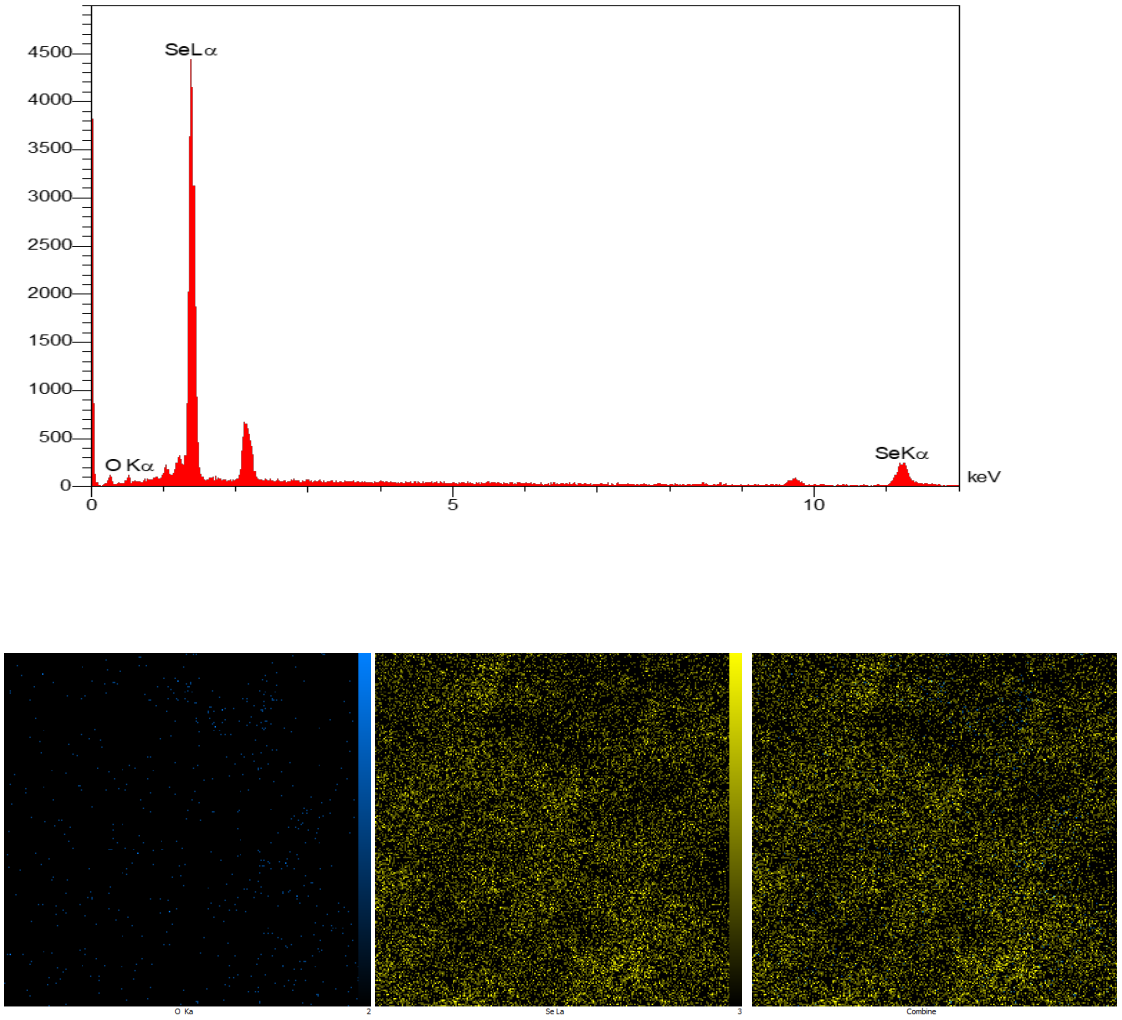

Fig. 4. EDX elemental mapping analysis of selenium nanoparticles (Se NPs) b) EDX spectrum of selenium nanoparticles (Se NPs).

peaks and valleys on the surface which shows that the nanoparticles were successfully nucleated and grown over the scanned surface area. The AFM data statistically showed that the prepared SeNPs have an average surface roughness (Ra) of ~40.91 nm and a root mean square roughness (Rq) of ~56.65 nm. The mean surface height was found to be almost 138.4 nm and the peak to valley roughness (Rp-v) was approximately 460.7 nm.These results indicate the formation of a highly textured nanostructured surface with significant surface irregularity.

Zeta potential distribution of Se NPS

Fig. 6 shows the zeta potential distribution of green-synthesized selenium nanoparticles (SeNPs) prepared using garlic extract as a natural reducing and stabilizing agent. The zeta potential profile

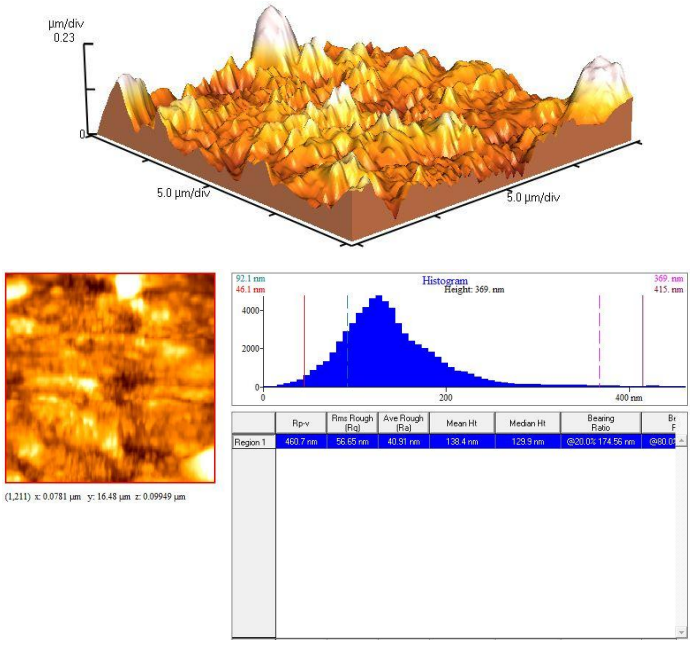

Fig. 5. AFM of Selenium nanoparticles (SeNPs).

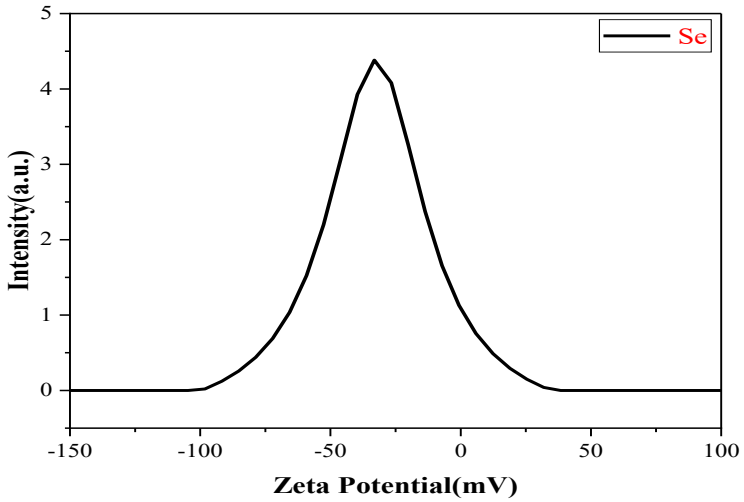

Fig. 6. Zeta potential distribution of Selenium nanoparticles (SeNPs).

exhibits a predominantly negative surface charge with the distribution centered approximately around -30 to -40 mV, indicating good colloidal stability of the synthesized nanoparticles in suspension. The negative values of zeta potential may be due to the adsorption of the negatively charged phytochemical compounds and sulfur containing functional groups of the garlic extract onto the surface of selenium nanoparticles. These bioactive molecules are natural capping and stabilizing agents that produce electrostatic repulsive forces between adjacent nanoparticles, which helps to reduce particle agglomeration. The large negative value of the zeta potential suggests the good stabilization of the SeNPs by the green synthesis method. The magnitude of the zeta potential is often used as a measure of the stability of the dispersion of nanoparticles in colloids; a zeta potential of at least ±30 mV is usually regarded as a good indicator of stable dispersion, because of the strong electrostatic repulsion between particles [34].

UV-Vis absorption

The UV-Vis absorption spectrum of green synthesized selenium nanoparticles (SeNPs) using garlic extract as natural reducing and stabilizing agent is shown in Fig. 7. The absorption spectrum

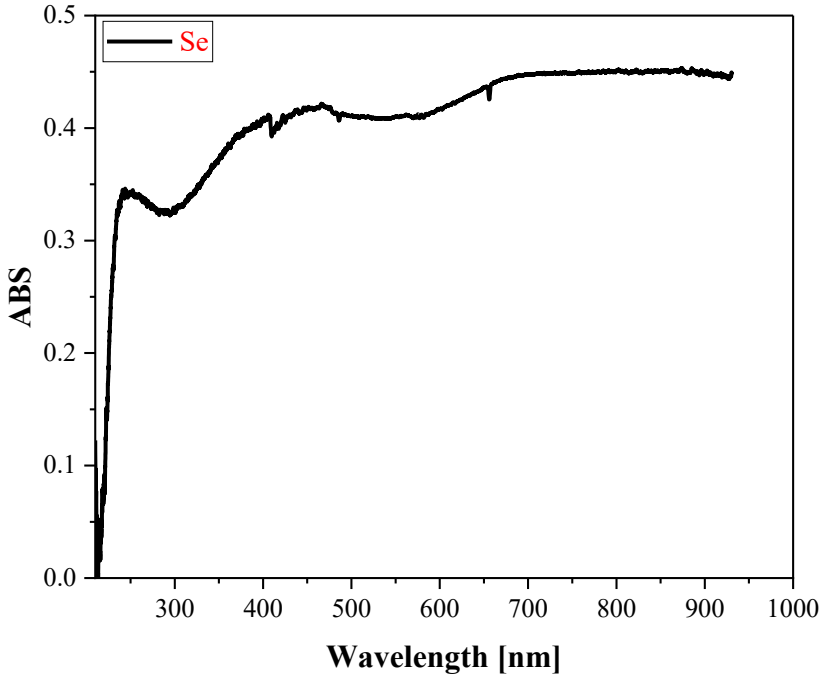

Fig. 7. UV-Vis absorption of Selenium nanoparticles (SeNPs).

Table 3. Antibacterial activity of green synthesized SeNPs against clinical isolates of E. coli measured by inhibition zone diameter (mm).

Isolate Code	500 mg/mL	250 mg/mL	125 mg/mL	62 mg/mL	32 mg/mL
E1	25	23	20	15	0
E2	10	8	9	0	0
E3	25	20	12	10	0
E4	0	10	11	0	0
E5	10	9	8	0	0
E6	14	12	12	10	8
E7	10	9	8	0	0
E8	13	11	10	8	0
Mean	13.38	12.75	11.25	5.38	1.00

shows that the optical absorption is strong in the ultraviolet region and gradually increases towards the visible region, which is indicative of the successful formation of selenium nanostructures. The observed optical behavior is mainly attributed to the electronic transitions within the selenium nanoparticles as well as the nanoscale effects associated with quantum confinement. A wide absorption band can be seen in the wavelength range of 250-350 nm, which is typical of selenium nanoparticles and is attributed to interband electronic transitions. The progressive shift of absorption towards the visible region indicates the presence of localized surface states and defect related energy levels created during the green synthesis process. These defect states are typically related to surface defects, vacancies, and the interaction between selenium nanoparticles and phytochemicals from garlic extract [35]. The relatively smooth and broad absorption profile also suggests the nanoscale nature and semi-uniform particle distribution of the synthesized SeNPs, which is in agreement with FESEM and XRD analysis. The improved absorption properties could be explained by the high surface to volume ratio of the nanoparticles and the presence of the organic capping molecules which are adsorbed on the surface of the nanoparticles [36]. The optical response of the prepared SeNPs shows that they can be used in biomedical, antibacterial, and photocatalytic applications, where high surface activity and strong light interaction are required.

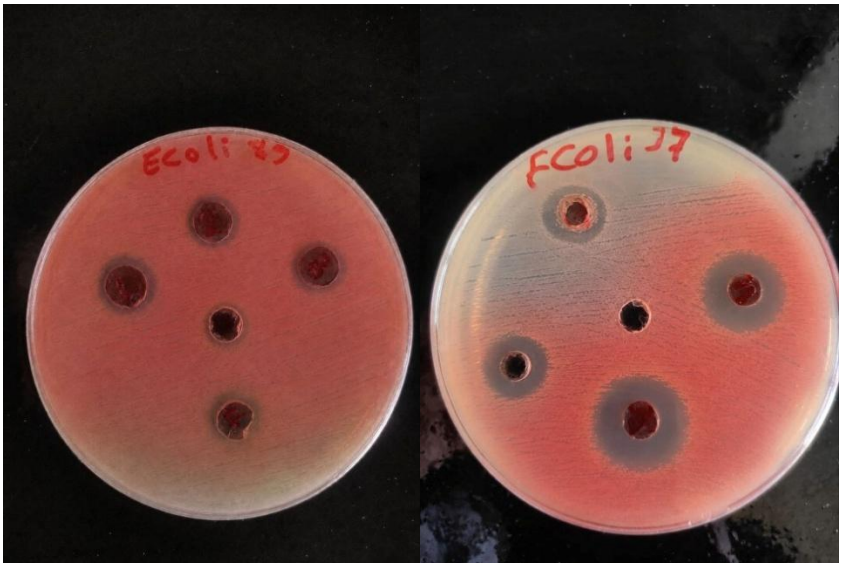

Fig. 8. Antibacterial activity of SeNPs against clinical isolates of E. col.

Table 4. Antibacterial activity of green synthesized SeNPs against clinical isolates of S. aureus measured by inhibition zone diameter (mm).

Isolate Code	500 mg/mL	250 mg/Ml	125 mg/mL	62 mg/mL	32 mg/mL
Isolate 1	20	15	13	10	0
Isolate 2	50	55	65	10	8
Isolate 3	0	0	25	0	0
Isolate 4	15	17	15	0	0
Isolate 5	23	20	15	0	0
Isolate 6	15	20	35	15	12
Isolate 7	50	40	45	17	15
Isolate 8	22	20	16	0	0
Mean (mm)	27.50	23.37	28.62	6.50	4.37

Antibacterial Activity by Biological Method

Antibacterial activity of selenium Nanoparticles Against Escherichia coli

The antibacterial activity results presented in Table 3 demonstrated that the green-synthesized selenium nanoparticles (SeNPs) prepared using Allium sativum extract exhibited variable inhibitory effects against the clinical isolates of E. coli obtained from wounds and burn infections. The inhibition zone diameter increased progressively with increasing nanoparticle concentration, confirming a concentration-dependent antibacterial activity. The highest antibacterial performance was observed at 500 mg/mL, whereas several isolates exhibited weak or no inhibition at lower concentrations, particularly at 32 mg/mL.

Antibacterial Activity of Se NPS Against Staphylococcus aureus

The inhibitory activity of the green-synthesized selenium nanoparticles (SeNPs) was also studied against clinical isolates of Staphylococcus aureus (S. aureus) obtained from traumatic wounds, surgical wounds, pressure sores and burn infections. The results shown in Table 4 indicated that the prepared SeNPs had significant antibacterial activity against majority of the isolates tested. The inhibition zone diameter was found to be increasing with the

Fig. 9. Antibacterial activity of green synthesized SeNPs against S.aureus isolate.

Table 5. Biofilm forming ability of clinical E. coli isolates.

Isolate Code	R1	R2	R3	Average	Biofilm Classification
Isolate 1	0.39	0.40	0.404	0.398	Strong
Isolate 2	0.63	0.65	0.646	0.642	Strong
Isolate 3	0.57	0.58	0.584	0.578	Strong
Isolate 4	0.72	0.73	0.737	0.729	Strong
Isolate 5	0.62	0.63	0.625	0.625	Strong
Isolate 6	0.60	0.61	0.617	0.609	Strong
Isolate 7	0.41	0.42	0.412	0.414	Strong
Isolate 8	0.47	0.48	0.487	0.479	Strong

increase in the concentration of nanoparticles, which indicated the concentration dependent antibacterial behavior of the nanoparticles. At intermediate concentrations, some isolates exhibited irregular responses, possibly due to the heterogeneous resistance properties of clinical isolates from different wound environments.

Biofilm Forming Ability of Clinical Escherichia coli Isolates

Table 5 showed that all E. coli isolates had a strong ability to form biofilms based on the OD595 readings from the standard microtiter plate assay. All the tested isolates had high adhesion capacity and produced a dense extracellular matrix, as the average OD values of all the tested isolates were significantly greater than the control classification limit.

Isolate 4 showed the highest ability to form biofilm with an average OD value of 0.729, followed by Isolate 2 (0.642) and Isolate 5 (0.625). Isolate 1, on the other hand, produced the least amount of biofilm among the isolates studied, but still fell within the strong biofilm producing range. The variation observed among the isolates is due to the difference in the virulence behavior, adhesion efficiency, production of extracellular polymeric substance (EPS) and adaptive resistance mechanisms of the bacteria.

Biofilm Forming Ability of Clinical Staphylococcus aureus Isolates

The results in Table 6 showed that all clinical Staphylococcus aureus isolates were strong biofilm formers based on the OD595 values obtained by the standard microtiter plate assay. All the isolates investigated had an average OD value that was significantly higher than the control OD value, which indicated that the tested isolates had a strong adhesion ability and produced a large amount of extracellular biofilm matrix.

Isolate 778 showed the highest biofilm forming ability with an average OD of 0.820 followed by Isolate 39 with an average OD of 0.750 and Isolate 546 with an average OD of 0.700. Isolate 445, on the other hand, had the lowest biofilm production of all the tested isolates, but still fell within the

Table 6. Biofilm forming ability of clinical Staphylococcus aureus.

Isolate Code	R1	R2	R3	Average	Biofilm Classification
Isolate 1	0.51	0.53	0.52	0.520	Strong
Isolate 2	0.74	0.76	0.75	0.750	Strong
Isolate 3	0.61	0.63	0.62	0.620	Strong
Isolate 4	0.48	0.49	0.50	0.490	Strong
Isolate 5	0.69	0.71	0.70	0.700	Strong
Isolate 6	0.57	0.59	0.58	0.580	Strong
Isolate 7	0.81	0.83	0.82	0.820	Strong
Isolate 8	0.66	0.68	0.67	0.670	Strong

Table 7. Antibiofilm activity of selenium nanoparticles (SeNPs) against clinical E. coli isolates.

Isolate Code	Treatment Mean OD630	Control Mean OD630	Biofilm Inhibition (%)
Isolate 1	0.086	0.142	39.25
Isolate 2	0.091	0.122	25.41
Isolate 3	0.099	0.101	1.64
Isolate 4	0.082	0.090	8.49
Isolate 5	0.083	0.087	4.60
Isolate 6	0.084	0.089	5.62
Isolate 7	0.092	0.120	23.33
Isolate 8	0.099	0.118	16.01

Table 8. Antibiofilm activity of SeNPs against E. coli.

Experimental Group	Mean ± SD (OD595)	Inhibition (%)
Positive Control	0.1089 ± 0.0237	0
SeNPs Treatment (590 µg/mL)	0.0898 ± 0.0086	17.49

strong biofilm producer category. The variation among the isolates suggests that the clinical strains vary in their adhesion ability, virulence characteristics, EPS production, and adaptive resistance mechanisms.

Antibiofilm Activity of SeNPs Against Escherichia coli

The results shown in Table *8* indicated that the green synthesized selenium nanoparticles (SeNPs) showed variable antibiofilm activity against the clinical isolates of E. coli. The treated groups showed a significant decrease in OD630 values when compared to the untreated controls, suggesting that the prepared SeNPs were able to inhibit the formation of biofilm and the adhesion of bacteria on the surface.

Isolate 1 showed the highest antibiofilm activity with a biofilm inhibition value of 39.25%, followed by Isolate 2 (25.41%) and Isolate 7 (23.33%). Isolate 3, on the other hand, showed the least anti-biofilm activity with only 1.64% inhibition, suggesting that the biofilm structure was highly resistant to the nanoparticles. This diversity among the isolates is due to the differences in extracellular polymeric substance (EPS) density, adhesion ability, membrane composition and adaptive resistance behaviour of the clinical strains.

Antibiofilm Activity of SeNPs Against Staphylococcus aureus

The results presented in Table 9 and Table 10 demonstrated that the green-synthesized selenium nanoparticles (SeNPs) exhibited significant

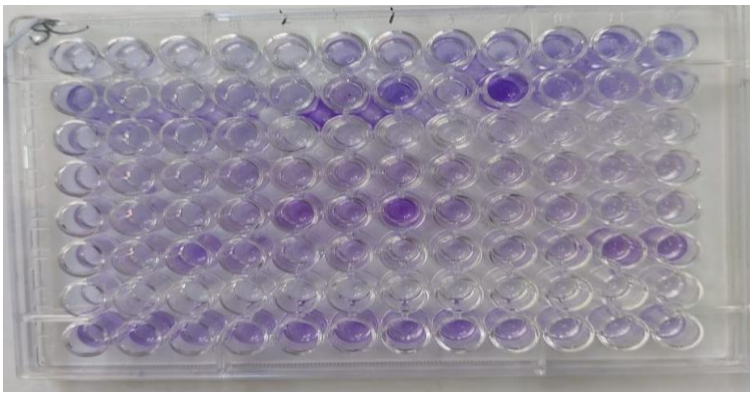

Fig. 10. Antibiofilm activity of selenium nanoparticles (SeNPs) against Staphylococcus aureus isolates and *Escherichia coli*.

Table 9. Antibiofilm activity of selenium nanoparticles (SeNPs) against clinical Staphylococcus aureus isolates.

Isolate Code	Treatment Mean OD595	Control Mean OD595	Biofilm Inhibition (%)
Isolate 1	0.074	0.128	42.18
Isolate 2	0.069	0.141	51.06
Isolate 3	0.082	0.133	38.34
Isolate 4	0.091	0.137	33.58
Isolate 5	0.073	0.149	51.01
Isolate 6	0.087	0.139	37.41
Isolate 7	0.066	0.152	56.58
Isolate 8	0.079	0.145	45.51

Table 10. Antibiofilm activity of SeNPs against Staphylococcus aureus.

Experimental Group	Mean ± SD (OD595)	Inhibition (%)
Positive Control	0.1708 ± 0.1352	0
SeNPs Treatment	0.1086 ± 0.0336	36.42

antibiofilm activity against the clinical isolates of *Staphylococcus* aureus. The OD595 values of the treated groups decreased markedly compared with the untreated control groups, confirming that the prepared SeNPs effectively suppressed biofilm formation and reduced bacterial surface adhesion (Fig. 10).

The Antibacterial Activity of Selenium Nanoparticles (SeNPs) against Ecoli

The present findings are consistent with those of Tran *et al*. (2022) [37], who found that selenium nanoparticles have measurable antibacterial activity against Gram-negative bacteria. This antibacterial effect is primarily characterized by membrane disruption, increased membrane permeability, and interference with intracellular metabolic processes.

However, the current findings differ from those reported by Fardsadegh and Jamebozorgi (2018) [38], who found that selenium nanoparticles had higher antibacterial activity against *E. coli*. This difference can be attributed to differences in nanoparticle physicochemical properties such as particle size, morphology, surface charge, and synthesis method. Furthermore, differences between bacterial strains and experimental conditions can have a significant impact on the antibacterial response. The lower susceptibility of *E. coli* in the present study may also be related to the presence of an outer lipopolysaccharide-rich membrane, which acts as a protective barrier and reduces nanoparticle penetration into bacterial cells.

Antibacterial Activity of Selenium Nanoparticles (SeNPs) Against Staphylococcus aureus

The current finding is also consistent with the work of Cremonin *et al* (2016) [39], who reported that gram-positive bacteria are generally more susceptible to selenium nanoparticles than gram negative bacteria. This behavior can be explained by the absence of an outer lipopolyscaccharied membrane in *S. aureus*, allowing easier access of nanoparticles to the bacterial cell wall and enhancing membrane disruption and oxidative damage.

On other hand, the present study dose not agree with the finding reported by Fardsadegh and Jamebozorgi (2018) [38], who observed different antibacterial responses of selenium nanoparticles against *S. aureus* and *E.coli*, with variable susceptibility depending on the nanoparticle characteristics and bacterial strain. Such discrepancies may be attributed to differences in nanoparticles size, morphology, surface charge, synthesis method and experimental conditions. In addition, varations in bacterial cell wall composition and resistance mechanisms among clinical isolates may influence the antibacterial efficiency of Se NPs.

Biofilm Formation by Clinical E. coli Isolates

The variation observed among the tested isolates may reflect differences in bacterial virulence behavior, adhesion efficiency, extracellular polymeric substance (EPS) production, and adaptive resistance mechanisms. The strong biofilm-forming capability observed in the present study can be associated with the clinical origin of the isolates obtained from wounds and burn infections. Burn-associated bacterial isolates are commonly exposed to prolonged hospitalization, repeated antibiotic treatments, oxidative stress conditions, and extensive tissue damage, all of which contribute to the development of highly adaptive bacterial populations capable of producing dense and highly protective biofilms. This agreement with Maitz, *et al (*2022) [40].

Biofilm Formation by Clinical Staphylococcus aureus Isolates

The differences observed among the isolates indicate variability in adhesion efficiency, virulence behavior, extracellular polymeric substance (EPS) production, and adaptive resistance mechanisms among the clinical strains. The remarkably strong biofilm formation observed in the present study linked to the clinical origin of the isolates obtained from wounds, burns, traumatic injuries, and surgical infections. *Staphylococcus* aureus is well known for its exceptional ability to colonize damaged tissues and form dense biofilms on biological surfaces. This agreement with Idrees ,*et al* (2021) [41].

The ability of S. aureus to strongly adhere to surfaces and form multilayered biofilm communities is associated with several surface adhesion proteins and extracellular polysaccharide components that enhance bacterial aggregation and stabilization within the biofilm matrix. This agreement with Badge *et al* (2025) [37].

Antibiofilm Activity of Selenium Nanoparticles

(SeNPs) Against E. coli Isolates

The decrease in OD595 after treatment suggests that the prepared SeNPs were able to inhibit the formation of biofilm and decrease the adhesion of bacteria on the surface. The differences in antibiofilm activity of the tested isolates could be due to the differences in extracellular polymeric substance (EPS) density, adhesion capacity, membrane composition and adaptive resistance behavior of the clinical strains.

The antibiofilm activity of SeNPs may be due to their nanoscale size and high surface reactivity, which allows them to penetrate the extracellular biofilm matrix and directly interact with the bacterial cells inside the biofilm structure. The selenium nanoparticles might interfere with the architecture of the biofilm by destabilizing the membrane, inducing oxidative stress and interfering with the extracellular polysaccharides that stabilize the biofilm. Furthermore, SeNPs can disrupt the communication systems and surface adhesion of bacteria, which can help to prevent the formation of mature biofilms and bacterial aggregation. This agreement with Souza et al (2022) [42].

Antibiofilm Activity of Selenium Nanoparticles (SeNPs) Against Clinical Staphylococcus aureus

The differences in inhibition efficiency between the isolates could be attributed to the differences in extracellular polymeric substance (EPS) density, adhesion strength, biofilm maturity and adaptive resistance mechanisms of the clinical strains isolated from wounds and burns.

The prepared SeNPs showed a more potent antibiofilm activity against S. aureus than E. coli. This behavior is mainly due to the difference in the architecture of the bacterial cell wall between Gram positive and Gram-negative bacteria. S. aureus does not have the outer lipopolysaccharide-rich membrane that provides an extra permeability barrier as seen in E. coli. Therefore, SeNPs are more likely to interact with the bacterial surface and penetrate the extracellular matrix of the biofilm, leading to higher disruption of the stability of the biofilm and bacterial adhesion. This agreement with Cezar M. et al (2018) [43].

CONCLUSION

1- Allium sativum (Garlic) extract as a natural reducing and stabilizing agent to green synthesis of selenium nanoparticles (SeNPs).

2-The successful formation of highly crystalline, stable, and nanosized particles was confirmed by 2- comprehensive characterization using XRD, FESEM, AFM, FTIR, EDX, UV–Vis spectroscopy, and zeta potential analysis.

3-The average crystallite size of the synthesized SeNPs was found to be ~17.6 nm. Nanoparticles had good colloidal stability, homogeneous elemental distribution, and nanoscale morphology appropriate for biological applications.

4-Biological evaluation showed that SeNPs had a significant antibacterial activity against clinical isolates of Escherichia coli and Staphylococcus aureus.

5-All clinical isolates of E. coli and S. aureus showed strong biofilm-forming ability, highlighting their virulence and potential resistance to conventional antimicrobial therapy. SeNPs showed moderate antibiofilm activity against E. coli and high antibiofilm activity against S. aureus.

6-Overall, the results indicate that the green synthesized SeNPs have potential antibacterial and antibiofilm activity.

7- Selenium Nanoparticles are potential alternative strategies for controlling multidrug-resistant and biofilm associated infections, especially wound and burn infections.

CONFLICT OF INTEREST

The authors declare that there is no conflict of interests regarding the publication of this manuscript.

REFERENCES

1. Nanotechnologies. Plain language explanation of selected terms from the ISO/IEC 80004 series. BSI British Standards. http://dx.doi.org/10.3403/30280230u
2. Radousky HB, Liang H. Energy harvesting: an integrated view of materials, devices and applications. Nanotechnology. 2012;23(50):502001.
3. Nikolova M, Slavchov R, Nikolova G. Nanotechnology in Medicine. Drug Discovery and Evaluation: Methods in Clinical Pharmacology: Springer International Publishing; 2018. p. 1-14.
4. Jenan Atiyah G. Biomedical Applications of Chitosan Nanoparticles: A Comprehensive Review. World Journal of Experimental Biosciences. 2019:9-17.
5. Nanotechnology in Medicine: Wiley; 2021.
6. Abbas HS, Abou Baker DH, Ahmed EA. Cytotoxicity and antimicrobial efficiency of selenium nanoparticles biosynthesized by Spirulina platensis. Arch Microbiol. 2020;203(2):523-532.
7. Fardsadegh B, Vaghari H, Mohammad-Jafari R, Najian Y, Jafarizadeh-Malmiri H. Biosynthesis, characterization and antimicrobial activities assessment of fabricated selenium nanoparticles using Pelargonium zonale leaf extract. Green Processing and Synthesis. 2018;8(1):191-198.

8. Padmalochini S, Rajeshkumar S, Lakshmi T, Tharani M. Green synthesis of selenium nanoparticles using clove and lemon grass and its antibacterial activity against E. faecalis. Journal of Complementary Medicine Research. 2022;13(5):90.
9. Tabibi M, Agaei SS, Amoozegar MA, Nazari R, Zolfaghari MR. Antibacterial, Antioxidant, and Anticancer Activities of Biosynthesized Selenium Nanoparticles Using Two Indigenous Halophilic Bacteria. Archives of Hygiene Sciences. 2020;9(4):275-286.
10. Kheradmand E, Rafii F, Yazdi MH, Sepahi AA, Shahverdi AR, Oveisi MR. The antimicrobial effects of selenium nanoparticle-enriched probiotics and their fermented broth against Candida albicans. DARU Journal of Pharmaceutical Sciences. 2014;22(1).
11. Tran PA, Webster TJ. Antimicrobial selenium nanoparticle coatings on polymeric medical devices. Nanotechnology. 2013;24(15):155101.
12. Dhanraj G, Rajeshkumar S. Anticariogenic Effect of Selenium Nanoparticles Synthesized Using Brassica oleracea. Journal of Nanomaterials. 2021;2021:1-9.
13. Nguyen THD, Vardhanabhuti B, Lin M, Mustapha A. Antibacterial properties of selenium nanoparticles and their toxicity to Caco-2 cells. Food Control. 2017;77:17-24.
14. Dumore NS, Mukhopadhyay M. Antioxidant properties of aqueous selenium nanoparticles (ASeNPs) and its catalysts activity for 1, 1-diphenyl-2-picrylhydrazyl (DPPH) reduction. J Mol Struct. 2020;1205:127637.
15. Azam A, Ahmed, Oves, Khan, Habib, Memic A. Antimicrobial activity of metal oxide nanoparticles against Gram-positive and Gram-negative bacteria: a comparative study. International Journal of Nanomedicine. 2012:6003.
16. Happy A, Soumya M, Venkat Kumar S, Rajeshkumar S. Mechanistic study on antibacterial action of zinc oxide nanoparticles synthesized using green route. Chemico-Biological Interactions. 2018;286:60-70.
17. Javanmard Z, Pourhajibagher M, Bahador A. Advancing Anti-Biofilm Strategies: Innovations to Combat Biofilm-Related Challenges and Enhance Efficacy. J Basic Microbiol. 2024;64(12).
18. Manning SD, Motiwala AS, Springman AC, Qi W, Lacher DW, Ouellette LM, et al. Variation in virulence among clades of Escherichia coli O157:H7 associated with disease outbreaks. Proceedings of the National Academy of Sciences. 2008;105(12):4868-4873.
19. Fleckenstein JM, Kuhlmann FM. Enterotoxigenic Escherichia coli Infections. Curr Infect Dis Rep. 2019;21(3).
20. Abu-Sini MK, Maharmah RA, Abulebdah DH, Al-Sabi MNS. Isolation and Identification of Coliform Bacteria and Multidrug-Resistant Escherichia coli from Water Intended for Drug Compounding in Community Pharmacies in Jordan. Healthcare. 2023;11(3):299.
21. Ravindra BM, Sadiya MR, Kiran PK, Raju KC. Pathogenic Escherichia coli (E. coli) food borne outbreak: Detection methods and controlling measures. Magna Scientia Advanced Research and Reviews. 2024;10(1):052-085.
22. Tigabu A, Getaneh A. Staphylococcus aureus, ESKAPE Bacteria Challenging Current Health Care and Community Settings: a Literature Review. Clinical Laboratory. 2021;67(07/2021).
23. Regev-Yochay G. Are methicillin-susceptible Staphylococcus aureus carriers protected from methicillin-resistant Staphylococcus aureus infections? Clinical Microbiology and Infection. 2019;25(1):4-5.
24. Laux C, Peschel A, Krismer B. Staphylococcus aureus Colonization of the Human Nose and Interaction with Other Microbiome Members. Microbiology Spectrum. 2019;7(2).
25. Cheung GYC, Bae JS, Otto M. Pathogenicity and virulence of Staphylococcus aureus. Virulence. 2021;12(1):547-569.
26. Linz MS, Mattappallil A, Finkel D, Parker D. Clinical Impact of Staphylococcus aureus Skin and Soft Tissue Infections. Antibiotics. 2023;12(3):557.
27. Peng Q, Tang X, Dong W, Sun N, Yuan W. A Review of Biofilm Formation of Staphylococcus aureus and Its Regulation Mechanism. Antibiotics. 2022;12(1):12.
28. Methicillin-resistant Staphylococcus aureus (MRSA). AccessScience: McGraw-Hill Professional.
29. Fait A, Silva SF, Abrahamsson JÅH, Ingmer H. Staphylococcus aureus response and adaptation to vancomycin. Advances in Microbial Physiology: Elsevier; 2024. p. 201-258. http://dx.doi.org/10.1016/bs.ampbs.2024.04.006
30. Mlynarczyk-Bonikowska B, Kowalewski C, Krolak-Ulinska A, Marusza W. Molecular Mechanisms of Drug Resistance in Staphylococcus aureus. Int J Mol Sci. 2022;23(15):8088.
31. Rajput P, Nahar KS, Rahman KM. Evaluation of Antibiotic Resistance Mechanisms in Gram-Positive Bacteria. Antibiotics. 2024;13(12):1197.
32. Determination of minimum inhibitory concentrations (MICs) of antibacterial agents by broth dilution. Clinical Microbiology and Infection. 2003;9(8):ix-xv.
33. Silva V, Almeida L, Gaio V, Cerca N, Manageiro V, Caniça M, et al. Biofilm Formation of Multidrug-Resistant MRSA Strains Isolated from Different Types of Human Infections. Pathogens. 2021;10(8):970.
34. Sam S, Fiol N, Aguado RJ, Saguer E, Carrasco F, Delgado-Aguilar M, et al. Green synthesis and optimization of selenium nanoparticles using chitosan or cationic cellulose nanofibers. Cellulose. 2024;32(2):919-940.
35. Structural and Optical Characterization of Luminescent Cd/Cu_{2-x}se Nanocomposites. Strad Research. 2020;7(10).
36. Gupta K, Chundawat TS. Time and Size-dependent Biogenically Synthesized Nanoparticles Using Fungus Fusarium Oxysporum: A Review on their Preparation, Characterization and Biological Activities. Nanoscience and Nanotechnology-Asia. 2020;10(2):95-108.
37. Webster TJ, Tran. Selenium nanoparticles inhibit Staphylococcus aureus growth. International Journal of Nanomedicine. 2011:1553.
38. Chemistry International CI. Green synthesis of copper oxide nanoparticles using Bougainvillea leaves aqueous extract and antibacterial activity evaluation. Center for Open Science; 2021. http://dx.doi.org/10.31219/osf.io/yqsk4
39. Cremonini E, Zonaro E, Donini M, Lampis S, Boaretti M, Dusi S, et al. Biogenic selenium nanoparticles: characterization, antimicrobial activity and effects on human dendritic cells and fibroblasts. Microb Biotechnol. 2016;9(6):758-771.
40. Maitz J, Merlino J, Rizzo S, McKew G, Maitz P. Burn wound infections microbiome and novel approaches using therapeutic microorganisms in burn wound infection control. Adv Drug Del Rev. 2023;196:114769.
41. Idrees M, Sawant S, Karodia N, Rahman A. Staphylococcus aureus Biofilm: Morphology, Genetics, Pathogenesis and Treatment Strategies. International Journal of Environmental Research and Public Health. 2021;18(14):7602.
42. Souza LMdS, Dibo M, Sarmiento JJP, Seabra AB, Medeiros LP, Lourenço IM, et al. Biosynthesis of selenium nanoparticles using combinations of plant extracts and their antibacterial activity. Current Research in Green and Sustainable Chemistry. 2022;5:100303.
43. Khursigara CM, Koval SF, Moyles DM, Harris RJ. Inroads through the bacterial cell envelope: seeing is believing. Can J Microbiol. 2018;64(9):601-617.